

# A Practical Approach for the Evaluation of Noise in Oscillator-Based Resistive Sensor Interfaces

Rafael Puyol<sup>1</sup>, Yannick Molle<sup>1</sup>, Sylvain Pétré<sup>1,2</sup>, Thomas Walewyns<sup>1,2</sup>, Laurent A. Francis<sup>1</sup>, Denis Flandre<sup>1</sup>

<sup>1</sup> Electrical Engineering Department (ELEN), ICTEAM Institute, Université catholique de Louvain (UCLouvain), Louvain-la-Neuve, Belgium

<sup>2</sup> VOCSens – Smart sensing solutions, Louvain-la-Neuve, Belgium

Corresponding author: denis.flandre@uclouvain.be

**Abstract**—Controlled oscillators are a leading option for sensor interfaces when high input dynamic range (DR) is needed. This is often met in applications like gas, temperature and strain sensing where the low level measurand is embedded in a high DC common-mode signal. Aiming for high DR and high accuracy, with low energy use, challenges the interface linearity and signal-to-noise ratio. Such performance requires the use of specific analytical tools for the design of the interface. In this article a methodology for the quantification of noise-related uncertainty in oscillator-based resistive sensor interfaces is presented. A time-domain analysis of the output oscillation is performed with the aid of classical period jitter tools and long-term stability is assessed with the Allan variance. Finally, an energetic evaluation constrained by the output requirements is carried out. As an application case, the methodology is used to evaluate the performance of a gas sensor interface confirming the need and usefulness of the proposed approach to achieve best accuracy.

**Keywords**—resistive sensor interface, jitter, Allan variance, IoT, electronics noise, polymer gas sensor

## I. INTRODUCTION

With the recent extensive deployment of IoT (Internet of Things) nodes, sensors have become very popular for monitoring and controlling environmental variables like air pollution, UV radiation, temperature and humidity to mention a few. Resistive sensors are the most frequently found type and the most challenging. For a single commercial device model, a large spread in its characteristics is possible due to the variability in the production process of sensing layers. For example a common metal-oxide gas sensor can have a baseline resistance variation of three decades and on top of this, two more decades in the sensing range (i.e. from 10 k $\Omega$  to 1.5 M $\Omega$  for a CCS801 sensor [1]). A dynamic range of 150 dB or more is not uncommon in these applications. It is very hard to tackle this problem using high-performance ADCs while still retaining the low power demanded by IoT applications. Oscillator based-interfaces where the output frequency is proportional to an input quantity, resistance, current or capacitance, are better suited [2][3].

In our study, the proposed methodology will be applied to the oscillator of Fig. 1. This digital oscillator works by integrating a current  $I_s$  (that is the result of biasing the sensor with a reference voltage  $V_{ref}$ ) on a capacitor  $C$ , until a threshold voltage is reached, then the current sign is reversed by means of switches (S) controlled by a Schmitt trigger. As

This work has been partly supported through the BioWin cluster BioCloud4.0 project funded by Wallonia, and through the MICRO+ project, co-funded by the European Regional Development Fund (ERDF) and Wallonia.

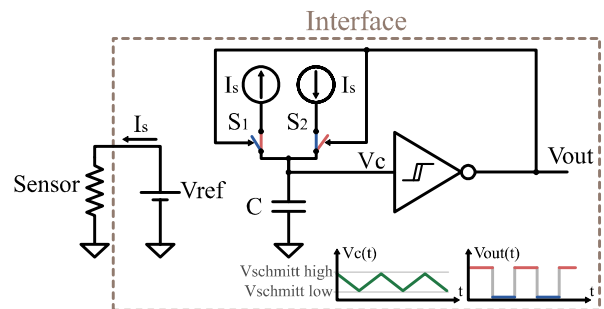


Fig. 1. Simplified schematic of an oscillator-based sensor interface,  $I_s$ , the sensed current, is copied to the integration capacitor by cascode current mirrors (not shown).

a result, the output frequency is proportional to the input current.

Given the voltage limitations of recent CMOS processes and the required large DR, the current of interest can get very small, in the order of nA or even pA. On top of this, for low-power consumption, transistors are usually biased in weak or moderate inversion, where they are more efficient at producing high gain, but at the same time, signals are weaker and uncertainty larger. Nonlinearities, process variations, mismatch and offset of the sensor and the circuit are major causes of uncertainty in the measurement but can be managed by calibration for each sensor. Consequently, the electronics noise coming from the sensor and the interface becomes dominant and is hence the focus of the present work.

Our aim is to provide reliable techniques to optimize the interface design both for best accuracy and low-power consumption. In section 2, the tools for the assessment of uncertainty, i.e. the jitter and the Allan variance, are presented. In section 3, the energy implications of the previous section are studied and finally in section 4, an application case is presented.

## II. TOOLS FOR MEASUREMENT UNCERTAINTY EVALUATION

### A. Jitter

Jitter is a measure of the deviation of the period of a periodic signal from its ideal value. It is a multicausal phenomenon, generated by random and deterministic processes. The most common are: thermal noise, flicker noise, electromagnetic interference, temperature variations and systematic deviations in the design.

Resistive sensors may add a considerable amount of thermal as well as flicker noise. In general, flicker noise is likely to be present in resistive sensors because typical sensed quantities like: gas concentration, temperature, humidity are slow-rate processes, in the milliseconds range. This has been confirmed by sensor measurements in [4], where only flicker noise was observed. Flicker noise in the sensor interface can be diminished by proper circuit design and zero-drift techniques, while on the other hand, the sensor noise cannot be dealt with in the same way. In all, no sensor interface will be optimal for every sensor and a characterization of the sensor noise power-spectral density (PSD) is needed for the evaluation of the different points of operation of the interface. As the oscillator operates in a wide range of frequencies, a plot of the jitter against period or frequency can help visualize the preferred operating region. After the sensor noise has been characterized, the plot can be obtained in two ways.

The first method is to approximate the sensor PSD by its flicker and thermal components and apply these sources to the input of the oscillator frequency model to calculate the jitter fraction of the period. This is done in eq. 1-3 for flicker and thermal sources separately. If the interface input noise values are also known, they can be added. In these equations,  $\beta$  is the current flicker noise proportionality constant,  $I_n$  is the square root of thermal current noise PSD,  $T$  is the oscillation period,  $Ci$  the cosine integral and  $V_{schmitt}$  the difference between the high and low threshold values. The development of these equations was done by modelling the interface as a linear system and resolving the integrals.

$$J_{thermal} = \frac{I_n}{\gamma} \sqrt{\frac{T\pi}{2}} \quad (1)$$

$$J_{flicker} = \sqrt{\frac{-\beta T(4T^2 Ci(2T) - 2T \sin(2T) + \cos(2T) - 1)}{2\gamma^2 \pi}} \quad (2)$$

$$\gamma = \frac{2CV_{schmitt}}{V_{ref}} \quad (3)$$

The second approach is more practical: the jitter chart can be obtained from simulations using the empirical sensor noise model. Some circuit simulators, like Eldo from Mentor Graphics, offer fast steady-state transient noise simulations, but it is also possible to obtain the jitter value from the eye diagram generated from time-consuming noise transient simulations. Moreover, an eye diagram provides a means for identifying non-random sources of jitter. An explanation of the distribution decomposition can be found in [5].

From the jitter frequency plot, the region of operation for a desired uncertainty level is immediately seen. To improve the accuracy and reduce the uncertainty introduced by jitter, averaging of two or more samples is frequently employed, at the cost of multiplying the required energy by the same factor. For some random process, like flicker noise, averaging does not always guarantee that the SNR will improve. As the time window is expanded, the high-pass effect is diminished letting more low frequency noise in. To study the effect of averaging, the Allan Variance is preferred.

### B. Allan Variance

Even though in the field of precise time metrology, the use of Allan variance is ubiquitous, it has rarely been used to

study oscillator-based sensor interfaces [6]. The Allan variance is calculated as a function of moving averages instead of using the ensemble average, which depends on the ensemble length [7]. For a set of  $N$  measurements of  $x(t)$ , the time deviation from an ideal periodic signal, the Allan variance is calculated as in eq. 4. The variance is a function of  $\tau$ , which is the product of the oscillation period  $\tau_0$  by an integer  $m$ .

$$\sigma_y^2(\tau) = E[(\bar{x}_{k+m} - \bar{x}_k)^2] = \frac{1}{2(N-2m)(m\tau_0)^2} \sum_{i=0}^{N-2m-1} (x_{i+2m} - 2x_{i+m} + x_i)^2 \quad (4)$$

Plotting the variance as a function of  $m$  provides a good insight of the noise characteristic of the oscillator. It is well understood that the slope of the Allan variance in the plots, correlates to the noise source PSD by eq. 5 [7] where  $h$  is the transfer function and  $\alpha$  the exponent of the noise process according to table 1.

$$S_y(f) = h(\alpha) \square f^\alpha \quad (5)$$

The Allan variance can also prove useful when testing the system, correlated noise sources can be identified, and their effects removed as explained in [8].

TABLE I. ALLAN VARIANCE EXPONENTS

Alpha	Process
-2	Random Walk FM
-1	Flicker FM
0	White FM
1	Flicker PM
2	White PM

### III. ENERGY CONSTRAINTS

After performing the noise analysis, the energy per conversion cycle has to be related to SNR. The current drawn by a resistive sensor system, can be separated into two components, one that is static or independent of the sensor resistance and another which is proportional. The energy per conversion cycle for the system is expressed in eq. 6, where  $I_s$  is the static current consumption of the interface,  $V_{dd}$  is the supply voltage and  $\gamma$ ,  $T$  and  $V_{ref}$  have been defined previously:

$$E(t) = V_{dd} \square (T \square I_s + \gamma \square V_{ref}) \quad (6)$$

### IV. EXPERIMENTAL CASE STUDY

In this section, the analytical tools presented before are applied to a system formed by a polypyrrole-based resistive sensor for sensing volatile organic compounds [4], and an integrated oscillator we designed an interface based on the architecture of Fig. 1 and under fabrication in UMC 0.18  $\mu\text{m}$  technology (fig. 2). The interface parameters are chosen as:  $C = 3$  pF,  $V_{schmitt} = 1$  V,  $V_{ref} = 1$  V, resulting in  $\gamma = 6$  pF. For the polypyrrole sensor, only flicker noise with  $\beta = 1$  fA<sup>2</sup> was observed in [4], but a theoretical sensor with only thermal noise will also be considered for completeness, with  $I_n = 1 \times 10^{-19}$  A<sup>2</sup>/Hz.

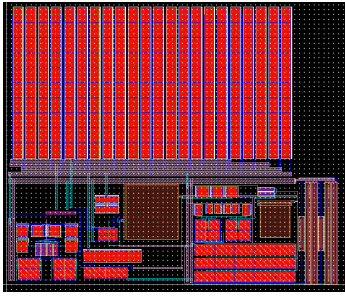


Fig. 2. Layout of the interface, area = 350 $\mu$ m x 300 $\mu$ m

In Fig. 3, the jitter fractions versus period are obtained using the two approaches of section II.A, i.e. from the models according to equations 1 and 2, and from simulations. The interface noise is less significant than that of the sensor, so in this case, the sensor noise model alone is sufficient to make a reasonable estimation of jitter. This again, supports the need for a proper sensor characterization as a starting point. In all, both ways deliver acceptable results, within the right order of magnitude. For both polypyrrole and theoretical sensors, it is seen that jitter increases with period, but more steeply when 1/f noise dominates.

The Allan variance plot is presented in Fig. 4, for a fixed oscillating period of 15  $\mu$ s and time traces obtained with noise transient simulations. The sensor interface noise is present in the three curves. Two straight lines were added to Fig. 4, with slopes -1 and 0 that fit very well the Allan variances for the sensors with flicker and thermal noise respectively, as predicted by table 1. For the gas sensor with flicker noise, the variance does not diminish for larger m, making averaging fruitless. On the other hand, averaging does help when the sensor noise is mostly thermal.

From eq. 6, it is seen that the energy dissipated in the sensor is constant for all periods, but that consumed by the interface is directly proportional to it. As a result, for shorter periods the sensor demands most of the energy for a given measurement, while for long periods the interface does. The theoretical corner of this phenomena for the oscillator under study is around 100 ns, but the minimum operating period of the oscillator is 1  $\mu$ s, meaning that the energy consumed in the interface is well above that of the sensor for the whole operational range. Besides this, eq. 6 is monotonically increasing, which means that the longer the period the higher the energy needed. As an example, in this oscillator, the energy per conversion cycle is 288 pJ for 1 $\mu$ s conversions, 1.91 nJ for 10  $\mu$ s and at 18.1 nJ for 100  $\mu$ s. This means that, even though the static current consumption of the interface is only 90  $\mu$ A, one of the lowest reported for this type of interfaces, further optimizations will significantly decrease the energy consumed per conversion cycle.

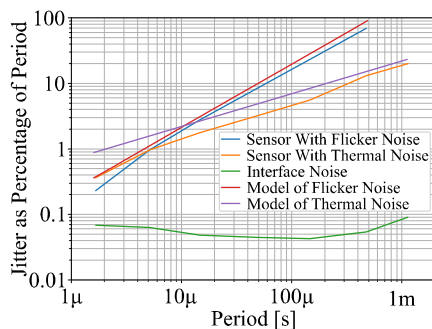


Fig. 3. Jitter as function of period for: the interface with the polypyrrole sensor, the interface with a theoretical sensor with only thermal noise and the interface alone.

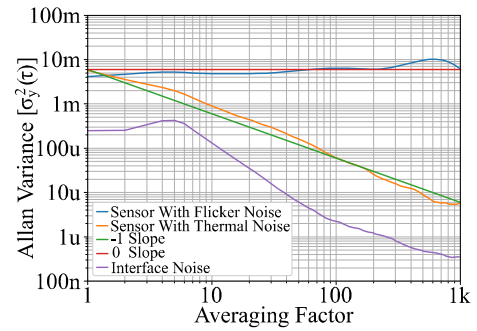


Fig. 4. Allan variance as function of the averaging factor for the system with: the polypyrrole sensor, a theoretical sensor with only thermal noise and the interface noise alone.

In Fig. 5, the jitter calculated as a percentage of the period is plotted in upper box and the gain in SNR (in dB) by averaging a certain number of samples is plotted in the lower box. Averaging should be pondered thoroughly as its effectiveness is strongly dependent on the noise process. In the example circuit, when the sensor exhibits only thermal noise, it takes 100 samples to gain 20 dB in SNR, increasing the energy.

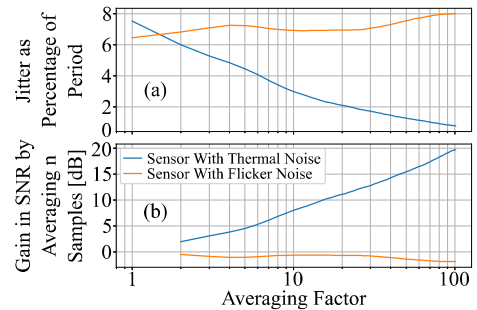


Fig. 5. (a) Jitter as function of averaging factor (b) Gain in SNR by averaging a given number of samples.

From the application of the methodology to this system, we see that in terms of jitter and energy, it is best to run the oscillator at the highest possible frequency. This presents the dilemma of running the oscillator at a suboptimal frequency to allow the positive and negative changes in the sensor from its initial value, or alternatively to adapt dynamically some parameters of the oscillator like,  $V_{ref}$ ,  $C$ ,  $V_{schmitt}$ , to maintain the oscillator near its optimal point, this is a decision that the designer should ponder as external requirements for concrete applications may come into play.

## V. CONCLUSIONS

We can conclude that jitter analysis coupled with the Allan variance provide a complete and precise method for studying the noise-related uncertainty of oscillator-based resistive sensor interfaces. We emphasize the need for sensor noise characterization as a starting point. This methodology was applied to a gas sensing system and the following results were found. Firstly, jitter estimations proved essential to find the optimal oscillating frequency, which in this example is 1 MHz with an uncertainty of 0.1 %. Secondly, from the Allan variance plot it can be stated that averaging is not beneficial when flicker noise is dominant in the frequency range of the oscillation. Finally, the energy consumption was estimated and shown to steadily decrease for higher oscillating frequencies, reaching a minimum of 288 pJ at 1 MHz, supporting even further, this region of operation.

## VI. REFERENCES

- [1] CCS801 Ultra-low power multi-gas sensor for indoor air quality, Cambridge CMOS Sensors Ltd, Deanland House, Cowley Road, Cambridge, UK.
- [2] F. Ciciotti, C. Buffa, V. Radogna, L. Francioso and S. Capone, "A 450- $\mu$ A 128-dB Dynamic Range A/D CMOS Interface for MOX Gas Sensors," in *IEEE Sensors Journal*, vol. 19, no. 24, pp. 12069-12078, Dec.15, 2019.
- [3] C. K. Leung and D. M. Wilson, "Integrated interface circuits for chemiresistor arrays," *IEEE International Symposium on Circuits and Systems*, Kobe, 2005, pp. 5914-5917 Vol. 6.
- [4] R. Puyol, S. Pétré, T. Walewyns, L. Francis and D. Flandre, "Design considerations of ultra-low power polymer gas microsensors based on noise analysis", *NanoFIS*, Graz, Austria, Nov. 2020.
- [5] N. Da Dalta and A. Sheikholeslami, "Basics of Jitter" in *Understanding Jitter and Phase Noise*, 1st edition, Cambridge, United Kingdom: Cambridge University Press, 2018, ch. 2, sec. 2.2.8, pp. 39-40.
- [6] Guan Chao, Li Xiujun and G. C. M. Meijer, "A system-level approach for the design of smart sensor interfaces," *SENSORS*, 2004 IEEE, Vienna, 2004, pp. 210-214 vol.1.
- [7] O. Baran and M. Kasal, "Allan variances calculation and simulation," 19th International Conference Radioelektronika, Bratislava, 2009, pp. 187-190.
- [8] M. Matejček and M. Šostronek, "New experience with Allan variance: Noise analysis of accelerometers," *Communication and Information Technologies (KIT)*, Vysoke Tatry, 2017, pp. 1-4.